Desalination and Water Treatment
www.deswater.com

doi:10.5004/dwt.2017.20797

79 (2017) 368–377
June

Decolourization of Methyl Orange (MO) by electrocoagulation (EC) using iron electrodes under a magnetic field (MF)

Sara Irki[a], Djamel Ghernaout[a,b,c,*], Mohamed Wahib Naceur[a]

[a]*Department of Chemical Engineering, College of Engineering, University of Blida, PO Box 270, Blida 09000, Algeria, email: irkirosa@gmail.com (S. Irki)*
[b]*Binladin Research Chair on Quality and Productivity Improvement in the Construction Industry, College of Engineering, University of Ha'il, PO Box 2440, Ha'il 81441, Saudi Arabia, Tel./Fax +213-25-433-631, email: djamel_andalus@hotmail.com (D. Ghernaout)*
[c]*Department of Chemical Engineering, College of Engineering, University of Ha'il, PO Box 2440, Ha'il 81441, Saudi Arabia, email: wnaceur@hotmail.com (M.W. Naceur)*

Received 6 November 2016; Accepted 6 April 2017

ABSTRACT

This work aims to treat the decolourization of methyl orange (MO) by the electrocoagulation (EC) method with application of a magnetic field (MF) (EC-MF). Experimentally, the electrochemical cell consists of two iron electrodes, which are kept at 2 cm with an active surface of 12.5 cm^2. The main experimental parameters, including supporting electrolyte, current density, pH and MO concentration, are optimized. After 12 min, the rate of MO decolourization by EC-MF reached its maximum (95%) which is higher than that obtained with EC (74%) at pH 7.25 with a current density of 64 A/m^2. The XRD analysis proved the presence of hematite Fe_2O_3 in the formed flocs. The SEM/EDX analysis confirmed the presence of iron and oxygen in the flocs. The removal mechanism suggested that MO be reduced to sulfanilic acid and 2-naphtol. The energy consumption was decreased from 28 to 19 kWh/kg of MO, for EC process and EC-MF, respectively. The obtained results depict that the application of the MF in the EC process is one of the most promising methods of increasing removal efficiency, accentuating process compactness and lowering energy consumption. More research is still needed to open the process of industrial application perspectives.

Keywords: Electrocoagulation (EC); Methyl orange (MO); Magnetic field (MF); Iron; Decolourization; Scanning electron microscopy (SEM); X-Ray diffraction (XRD); Supporting electrolyte (SE)

1. Introduction

The textile industry is one of the most important industries throughout the world. In the textile industry, the water consumption, especially in the dyeing and washing processes, is very high. As a result, large amounts of wastewater are produced and discharged into the receiving environment. In recent times, the use of organic dyes has been dramatically increased. Indeed, the azo dyes represent approximately 60–70% of the synthetic chemical dyes which are widely used in textiles [1–3]. Azo dyes producers and users are interested in stability and fastness of dyes on the fabric and they are continually producing azo dyes which are more difficult to degrade after use, and this also poses a problem for the natural degradation of azo dyes in the environment [4,5]. About 50000 tonnes of textile dyes are discharged into the environment annually from the dyeing process [6]. The release of these dyes into wastewater is harmful not only because of their colours but also due to the fact that many azo dyes are toxic to nature [7,8] and can be *carcinogenic* [9].

The electrocoagulation (EC) technique is considered versatile for the treatment of textile wastewaters [10–14]. This process is the electrochemical production of destabilization agents (such as Fe/Al) that bring about coagulation, the adsorption or the precipitation of soluble or

*Corresponding author.

colloidal pollutants [15–19]. A number of authors have reported the treatment of textile dye wastewaters by EC technique [14,15,20]. In addition, specific applications of EC have proved it as a promising process [16,21–23]. Although the textile dye wastewaters could be treated by some methods such as advanced oxidation processes, including UV/H_2O_2 and O_3 [24], and adsorption using activated carbon [25], the costs of these methods are relatively high for an economically feasible treatment of wastewater.

The effect of a magnetic field (MF) on electrochemical reactions has been the subject of many investigations [26–30]. These investigations were devoted to the study of diffusion of excess charge carriers in an MF. The application of MF on an electrochemical system allowed the introduction of additional forces to the solution ions. The first effect one will probably encounter is the magneto-hydrodynamic action; its origin is attributed to the Lorentz force [29]. It acts on moving charges by accelerating them in the direction perpendicular to the current and the flux density and thus leads to a stirring effect of the electrolyte. This action can significantly enhance the mass transport. This phenomenon will lead to an increase in the limiting current density because the thickness of the Nernst layer is reduced in the presence of a perpendicular MF [28,30].

Electrode position was carried out to study the effects of a homogeneous MF, with different strengths and orientations, on the deposition of Co, Fe and CoFe alloys. The results of these studies demonstrate that external homogeneous MF parallel to working electrode surface increases the limiting current densities and deposition rates [29]. The impact of external alternating MFs on suspended magnetic particles may lead to a forced and very intensive particle movement [31] and the precipitation process of calcium carbonate scale from hard water [32].

In the present work, we study the effect of MF on the decolourization of synthetic wastewater, methyl orange (MO), by an EC process using iron electrodes. These electrodes are chosen to increase the magnetic field application and Fe particles subsequent separation [27–30]. We are focusing on analyses of the flocs formed as well as the aqueous phase. Operating parameters, including electrolyte concentration, current density, pH, distance between the electrodes, and dye concentration, are investigated. The main EC process characteristics with and without MF are also compared.

2. Experimental

2.1. Experimental apparatus

The EC set-up with MF magnets used in our experiments is shown in Fig. 1. The EC unit was made of Plexiglas with the dimensions of 60 mm × 80 mm. There were two iron electrodes used, each one with dimensions of 50 mm × 25 mm × 2 mm, and the distance between them in the EC cell was fixed at 1 mm. The permanent magnets with 0.1 Tesla (T) were placed parallel to the cathode surface and the anode surface, respectively (Fig. 1). The electrodes were connected to a direct current (DC) power supply (Elektrolyser, type Elyn1) with an ammeter and voltmeter used in controlling the current and the voltage during the EC process, respectively. Before each run, the electrode plates were cleaned manually by abrasion with sandpaper and by treatment with 15% HCl acid followed by washing with distilled water.

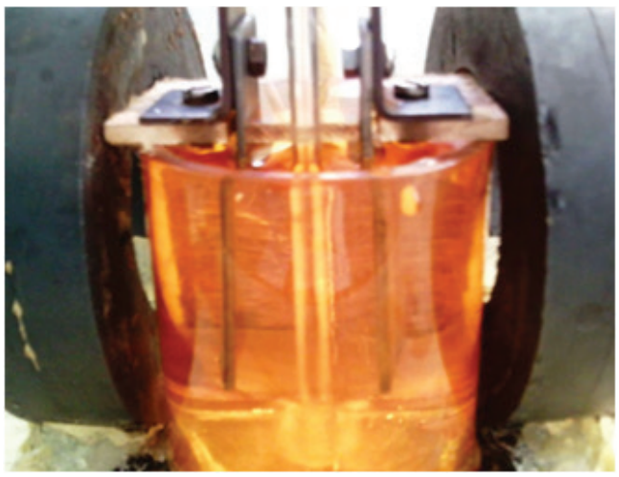

Fig. 1. The apparatus of EC with MF magnets placed for the treatment of MO.

2.2. Experimental procedure

The dye Orange III (abbreviated as methyl orange MO) is used for preparing wastewater solution by dissolving this organic compound in distilled water. The solution conductivity values were adjusted by adding NaCl as supporting electrolyte (SE) to the 200 mL solution of the synthetic wastewater. The pH of the tested solutions was measured by Hanna pH-meter and adjusted by adding HCL 0.05 N or NaOH 0.05 N. At the end of the EC experiments, all samples were filtered through a 0.45 µm pore size syringe filter. The MO concentration (C_{MO}) was measured using a Jenway Model 6800 SC Double Beam UV/Vis spectrophotometer at a wavelength corresponding to the maximum absorbance of the MO (l_{max} = 465 nm). The colour removal efficiency R (%) was calculated using Eq. (1), where Abs_i and Abs_f are initial and final absorbance, respectively:

$$R(\%) = \left(\frac{Abs_i - Abs_f}{Abs_i} \right) \times 100 \quad (1)$$

2.3. Scanning electron microscopy (SEM)

The surface morphology of the flocs was investigated using Scanning Electron Microscope (SEM), QUANTA 400 from FEI Company. The elemental composition was identified using energy disperses X-ray (EDX) analysis detector from EDAX system (a division of AMETEK). The samples were separated by decantation, then dried at the ambient air and ground to fine powder.

2.4. X-ray diffraction (XRD)

The X-ray diffraction (XRD) analysis is the most widely used technique in the identification of crystalline compounds and for both qualitative and quantitative analy-

sis. Our XRD measurements were carried out on an X'Pert PROP analytical diffractometer using filtered Cu Ka radiation (k = 0.1541 nm) at 2 range from 10 to 70.

3. Results and discussion

The effects of electrolyte concentration (C), MO concentration (C_{MO}), current density (J), and pH of the MO solution were investigated in order to determine the optimum operating conditions for the MO maximum removal efficiency.

3.1. Effect of the supporting electrolyte (SE) nature

The SE, consisting of anions and cations that are initially present in the solution or added in order to increase the solution conductivity, can potentially have considerable effects on (i) the rate of metal dissolution, (ii) the ohmic drop—and thus on the cell voltage and energy consumption, and (iii) surface phenomena occurring between polluting species and the metal hydroxides [33].

Figs. 2 and 3 present the effect of the SE on the EC performance in terms of dye removal and energy consumption. As illustrated in Fig. 2, the obtained results indicate that the removal efficiency depends on the SE types. Very high removal efficiencies were obtained in the range of 95 to 98% with chloride salt, potassium chloride and calcium chloride, whereas a lower removal efficiency of 79% was obtained using sodium sulphate. Besides, the experimental results depict that the sodium nitrate has a weak performance since its removal efficiency is only 16%. Some authors have found similar results about sodium nitrate [33].

Moreover, it has been found that chloride ions could significantly reduce the adverse effect of other anions such as HCO_3^- and SO_4^{2-} [34,35]. The existence of the carbonate or sulphate ions would lead to the precipitation of Ca^{2+} or Mg^{2+} ions that form an insulating layer on the surface of the electrodes [35].

The evolution of the SE effect as a function of time on the removal efficiency has been investigated at the same conditions as in Fig. 2 and illustrated in Fig. 3. The energy consumption (E) of the removed dye was calculated using Eq. (2) [36]:

$$E\left(kWh / kg\ of\ MO\right) = \frac{I \times t_{EC} \times U}{[C]_0 V \times 10^3} \quad (2)$$

where I is the current intensity (A), t_{EC} is the electrolysis time (h), U is the cell voltage (V), V is the volume of solution (m^3) and $[C]_0$ is the initial pollutant concentration (kg/m^3).

As shown in Fig. 3, it can be concluded that the lowest energy consumption for MO decolourization is about 21 kWh/kg of MO with NaCl; so NaCl may be considered as the most favourable SE. It is suggested that MF treatment causes changes in the hydrating water structure around the ions. These changes can be related to the presence of so-called structure – ordering or – disordering ions in the solution with NaCl [35].

3.2. Effect of NaCl concentration

The effect of electrolyte concentration was investigated between 0.3 and 2 g/L by using NaCl as the SE. Figs. 2 and 3 depict the effect of C_{NaCl} on the EC process. The results prove that the colour removal efficiency increased considerably from 68 to 91% at 12 min with increasing C_{NaCl} from 0.3 to 1 and then to 6 g/L. It was found that, when NaCl is added at 2 g/L to the dye solution, the colour removal efficiency rate decreases to 68%. For all the cases, it was found that the energy consumption decreases with increasing C_{NaCl}. The addition of sodium chloride would lead to the decrease in energy consumption because of the increase in conductivity. Although the maximum removal efficiency was achieved by adding 1.6 g/L of NaCl, the energy consumption was considerably reduced to 16 kWh/kg of MO.

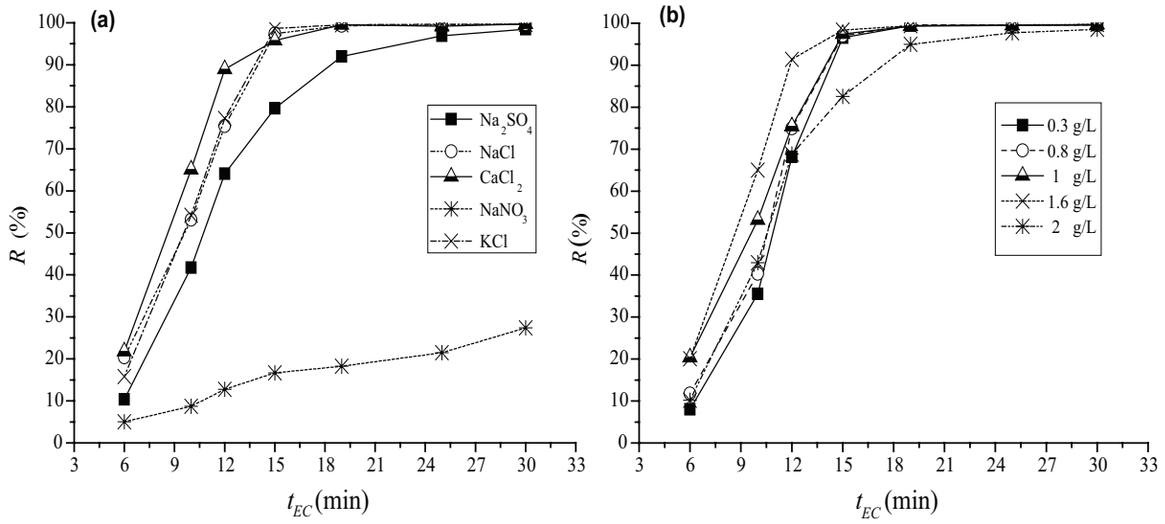

Fig. 2. (a) Effect of the SE nature on the removal efficiency of MO (C_{MO} = 15 mg/L, MF = 0.1 T, C_{NaCl} = 1 g/L, J = 64 A/m², d = 1 cm). (b) Effect of C_{NaCl} on the removal efficiency of MO (C_{MO} = 15 mg/L, MF = 0.1 T, J = 64 A/m², d = 1 cm).

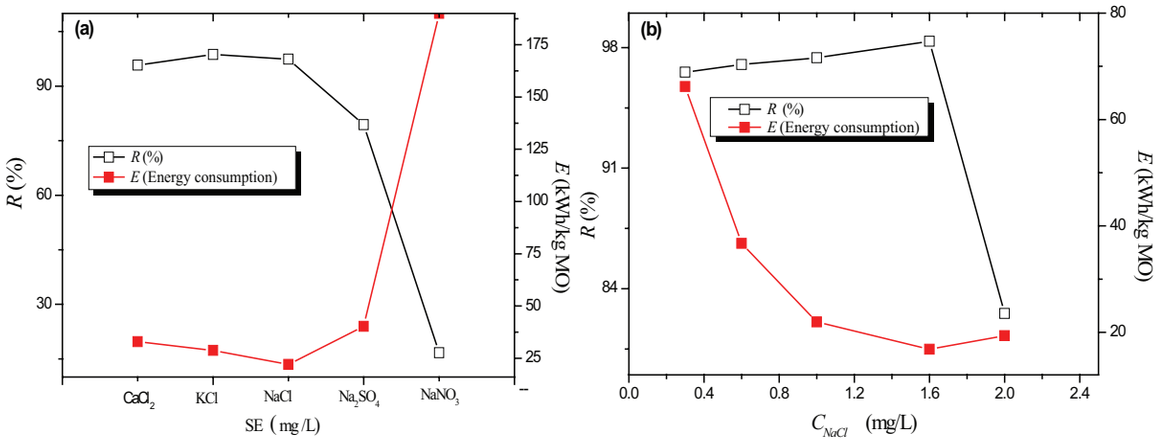

Fig. 3. (a) Effect of the SE type on the removal efficiency and consumption of energy (C_{MO} = 15 mg/L, MF = 0.1 T, J = 64 A/m^2, d = 1 cm, t_{EC} = 15 min). (b) Effect of C_{NaCl} on the removal efficiency and consumption of energy (C_{MO} = 15 mg/L, MF = 0.1 T, J = 64 A/m^2, d = 1 cm, t_{EC} = 15 min).

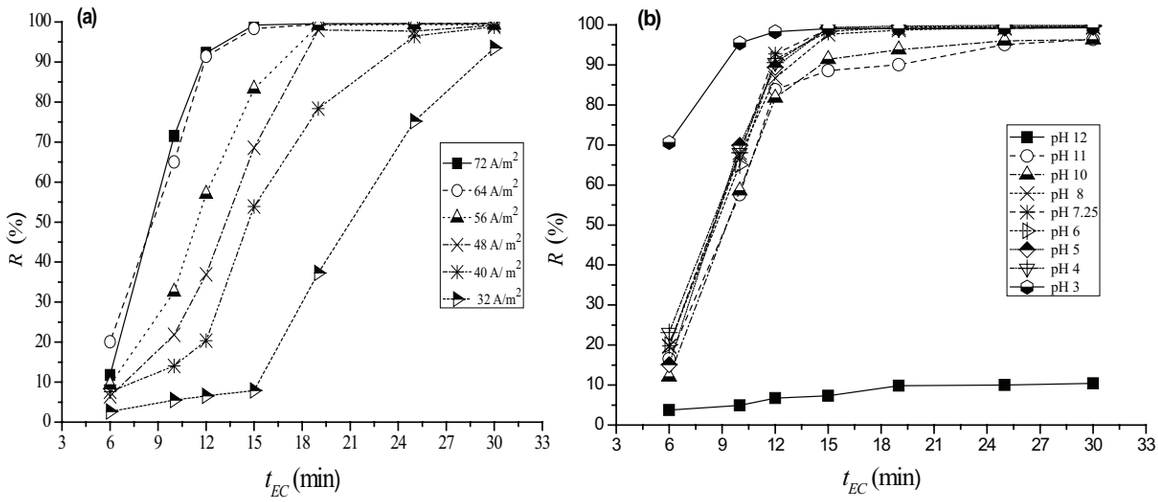

Fig. 4. (a) Effect of J on the removal efficiency of MO (C_{MO} = 15 mg/L, C_{NaCl} = 1.6 g/L, MF = 0.1 T, d = 1 cm). (b) Effect of pH on the removal efficiency of MO (C_{MO} = 15 mg/L, C_{NaCl} = 1.6 g/L, MF = 0.1 T, J = 64 A/m^2, d = 1 cm).

3.3. Effect of the current density

The effect of the current density (J) on the removal efficiency is illustrated in Figs. 4 and 5. The removal efficiency was increased from 7 to 99% when J was increased from 32 to 72 A/m^2. The results illustrated that the optimum removal efficiency of 98% was achieved at J = 64 A/m^2. Increasing J means that the amount of the electric current used in the electrochemical device is increased. In fact, J is the key operational parameter for the design of an EC device. It not only affects the system response time but also strongly influences the dominant pollutant separation mode [34].

In other words, the supply of J to the EC set-up directly determines both the amount of coagulant and bubble generation rates and strongly influences both solution mixing and mass transfer at the electrodes [37,38]. A large current means a small EC unit. However, very high J would lead to a significant decrease in current efficiency and waste electrical energy in heating up the water. It is necessary to control the current density to keep it below the limiting value with which to avoid the excess of hydrogen and chlorine when the pH is lowest [38,39]. Our results also depicted that energy consumption was increased from 7 to 15 kWh/kg of MO when the current density was higher than 40 A/m^2 (Fig. 5).

3.4. Effect of pH

The pH of the solution is an important factor influencing the performance of both the electrochemical and the chemical coagulation processes [38]. In order to investigate the effect of pH on the efficiency of colour removal, EC process experiments were carried out by using different initial pH values in the range of 3–12. The dye concentration of C_{MO} = 15 mg/L, C_{NaCl} = 1.6 g/L, and J = 64 A/m^2 were tested. The experimental results are presented in Figs. 4 and 5.

Fig. 4 shows that the initial pH has a significant effect on the removal efficiency of the dye. Indeed, when the pH of the dye solution was between 3 and 7, the removal efficiency was over 90%. Then the EC performance decreased to 83% when pH reached 11. The removal efficiency was particularly important in pH 7.25, for which it reached 92% at 12 min (Fig. 4). After EC treatment, pH would increase towards the alkaline interval when the initial pH was in the range of 3–11.

On the other hand, the energy consumption increased with the increase in pH values from 3 to 11: it augments from 15 to 18 kWh/kg of MO. Low energy consumption for the decolourization process was achieved at pH 7.25. Indeed, when decolourization efficiency reached 92% at pH 7.25, the energy consumption was 13 kWh/kg of MO. It can be deduced that the majority of iron complexes formed at pH between 3 and 9 are probably favourable for carrying out in the EC process. Ghernaout et al. [40] reported that the electromagnetic field application in continuous mode followed by EC in a batch has increased the removal efficiency until 100% when the pH of the humic acid solution was adjusted to 7.

3.5. Effect of the inter-electrode distance (*d*)

The effect of the inter-electrode distance (*d*) separating the anode from the cathode on the dye removal was varied from 0.8 to 3 cm, as shown in Figs. 6 and 7. From the obtained results, it appears that the high efficiency was recorded with a rate higher than 90% when *d* was increased from 0.8 to 2 cm. The removal efficiency decreases to 84% beyond 2 cm.

Our results proved also that the consumption energy increased from 13 to 31 kWh/kg of MO with an increase in *d* from 0.8 to 3 cm (Fig. 7). When the electrodes were main-

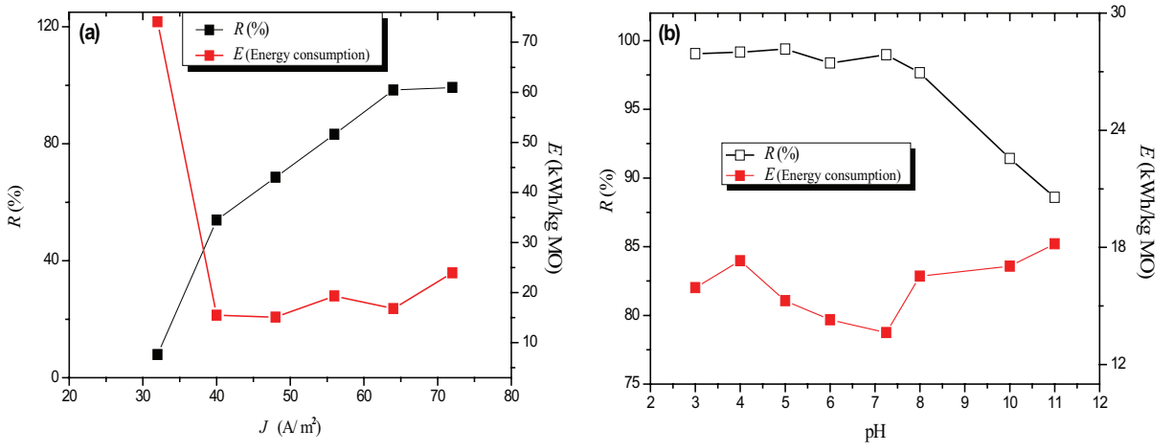

Fig. 5. (a) Effect of *J* on the removal efficiency and consumption of energy of MO (C_{MO} = 15 mg/L, MF = 0.1 T, C_{NaCl} = 1.6 g/L, *d* = 1 cm, t_{EC} = 15 min). (b) Effect of pH on the removal efficiency of MO (C_{MO} = 15 mg/L, C_{NaCl} = 1.6 g/L, MF = 0.1 T, *J* = 64 A/m², *d* = 1 cm).

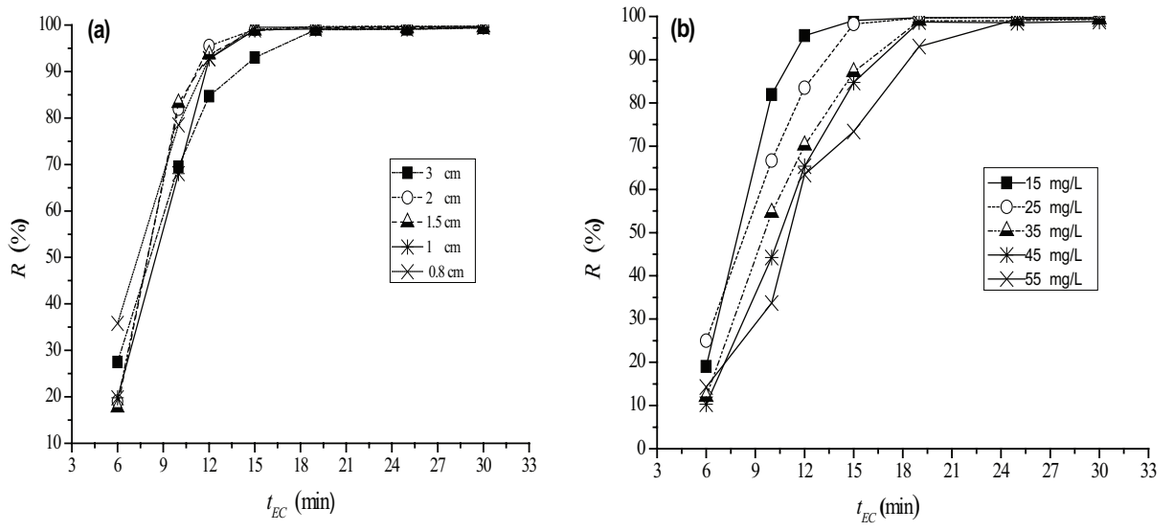

Fig. 6. (a) Effect of the inter-electrode distance on the removal efficiency of MO (C_{MO} = 15 mg/L, MF = 0.1 T, C_{NaCl} = 1.6 g/L, *J* = 64 A/m², pH = 7.25). (b) Effect of the initial MO concentration on the removal efficiency (C_{NaCl} = 1.6 g/L, MF = 0.1 T, *J* = 64 A/m², *d* = 2 cm, pH = 7.25).

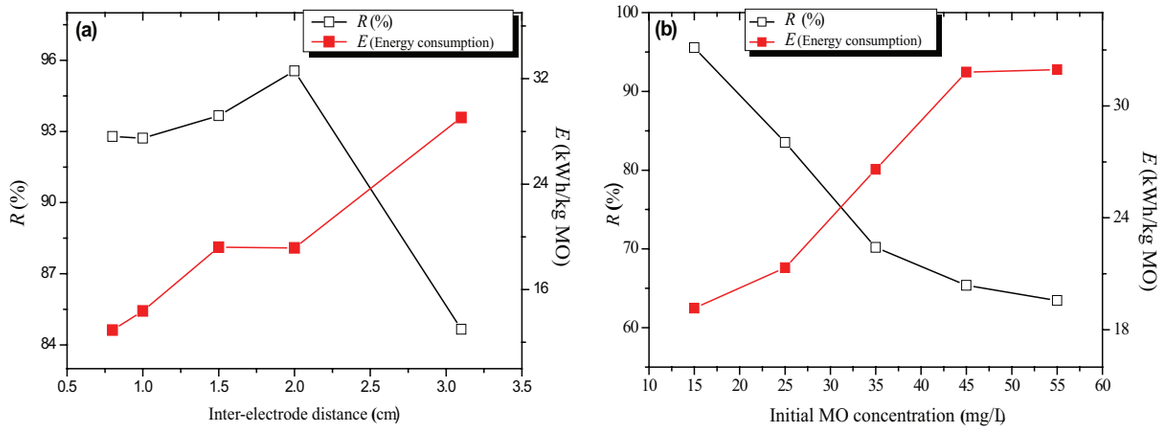

Fig. 7. (a) Effect of the inter-electrode distance on the removal efficiency and consumption of energy (MF = 0.1 T, C_{NaCl} = 1.6 g/L, J = 64 A/m², t_{EC} = 12 min). (b) Effect of the concentration on the removal efficiency and consumption of energy (MF = 0.1 T, C_{NaCl} = 1.6 g/L, J = 64 A/m², d = 2 cm, pH = 7.25, t_{EC} = 12 min).

tained at 2 cm, the removal efficiency of 95% was reached after 12 min, with energy consumption accounting for 19 kWh/kg of MO. These changes are attributed to the fact that the electrostatic effect depends on both d and MF; so when d was increased to 2 cm, the movement of ions in the MF presence was accelerated and the electrostatic attraction was increased. Consequently, the voltage would increase from 2.45 to 3.48 V for obtaining the optimum current density, which leads to an increase in the treatment efficiency.

3.6. The effect of the initial MO concentration

The dye solutions with different initial concentrations in the range of 15–55 mg/L were treated in the optimized conditions: current density (J = 64 A/m²), initial pH of 7.25, and C_{NaCl} = 1.6 g/L. As seen in Figs. 6 and 7, with the increase in the initial dye concentration, the removal efficiency is reduced. The removal efficiencies for the 15 and 55 mg/L concentrations both decreased from 95% to 60%, respectively, after 12 min; and then the rate reached only 70% for 55 mg/L, while the maximum rate reached 99% and 98% for 15 and 25 mg/L, respectively, after 15 min.

It was noticed that the energy consumption continuously went down. It was 19 kWh/kg of MO at C_{MO} = 15 mg/L, then increased for 29 kWh/kg of MO at C_{MO} = 55 mg/L. Based on the results obtained by the treatment of EC coupled with MF with 0.1 T, this combination of EC-MF was not effective in decolourizing the dye solution when the concentration of dye was greater than 35 mg/L. Consequently, the MF intensity was insufficient to produce flocs at high dye concentration.

3.7. Effect of the MF application

As illustrated in Fig. 8, the evolution of the removal efficiency by the treatment of EC with MF starts quickly and reaches 95% at 12 min. This rate is higher than that obtained with treatment by EC, which does not exceed 74%. Fig. 8 indicates that energy consumption with the application of MF reached 19 kWh/kg of MO, whereas it was 28 kWh/kg of MO without it. However, these results indicated that the application of MF in the EC was one of the most promising methods for lowering energy consumption.

3.8. Flocs characterization

The separation of the flocculated sludge formed by the EC process can be accomplished by precipitation after stopping the EC process. This approach is a relatively slow operation compared to the separation of the flocculated sludge in the presence of the MF.

SEM picture of the flocs obtained after treatment of EC coupled with MF revealed the formation of lumpy agglomerates of larger-sized particles; it appears that these flocs were irregular aggregates with a larger surface area (Fig. 10).

From Table 1, EDX analysis confirmed the presence of a very high amount of iron and oxygen with a weight percentage of 60.84% and 34.49%, respectively. Moreover, there is a low content of carbon of 3.26%, while the very low contents are for the sodium and chloride of 0.57% and 0.85%, respectively. Such a significant proportion of iron indicates the probable presence of hematite.

An XRD pattern is presented in Fig. 11 for flocs generated by the EC process with the application of the MF. The XRD spectrum presented high-intensity peaks and low-intensity peaks, which correspond to hematite (Fe_2O_3) in the most predominant crystalline phases.

On the other hand, the evolution of absorbance of MO solution as a function of time during the EC-MF process has occurred particularly in the visible range, but the degradation products can be usefully observed in the ultraviolet range (UV-Vis). Fig. 12 shows the UV-Vis spectrum of degradation of MO during EC-MF. The visible absorbance is at its maximum at 465 nm for MO. It decreases from 1 to 0.052 within 12 min. The evolution of the formation of the degradation product (N,N-dimethylaniline) is followed by measuring the absorbance at 248 nm (Fig. 12). The absorbance increases gradually from 0.1 to 0.87 within 12 min, then the absorbance will not change after 12 min, which corresponds to the accumulation of degradation products (Fig. 12).

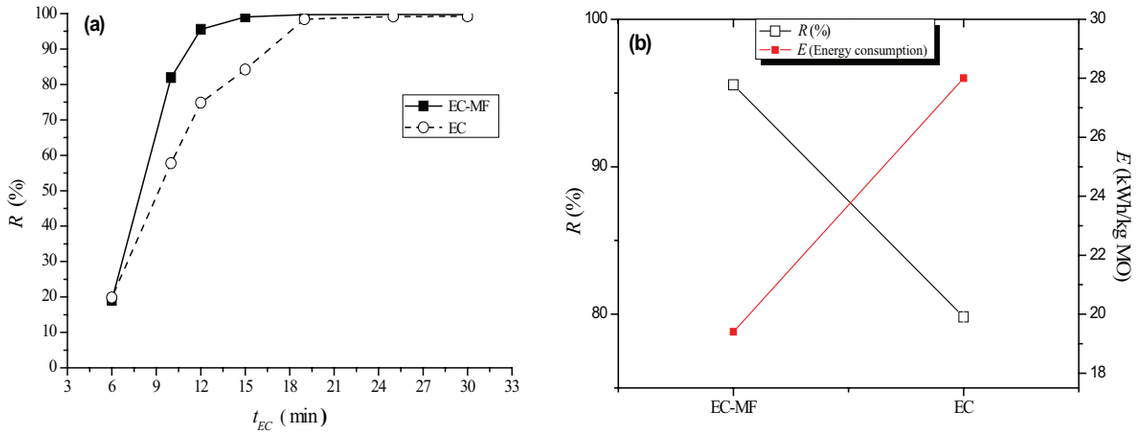

Fig. 8. (a) Effect of the MF on the removal efficiency of MO (C_{MO} = 15 mg/L, C_{NaCl} = 1.6 g/L, MF = 0.1 T, J = 64 A/m², d = 2 cm). (b) Effect of the MF on the removal efficiency and consumption of energy (C_{MO} = 15 mg/L, MF = 0.1 T, C_{NaCl} = 1.6 g/L, J = 64 A/m², d = 2 cm, t_{EC} = 12 min).

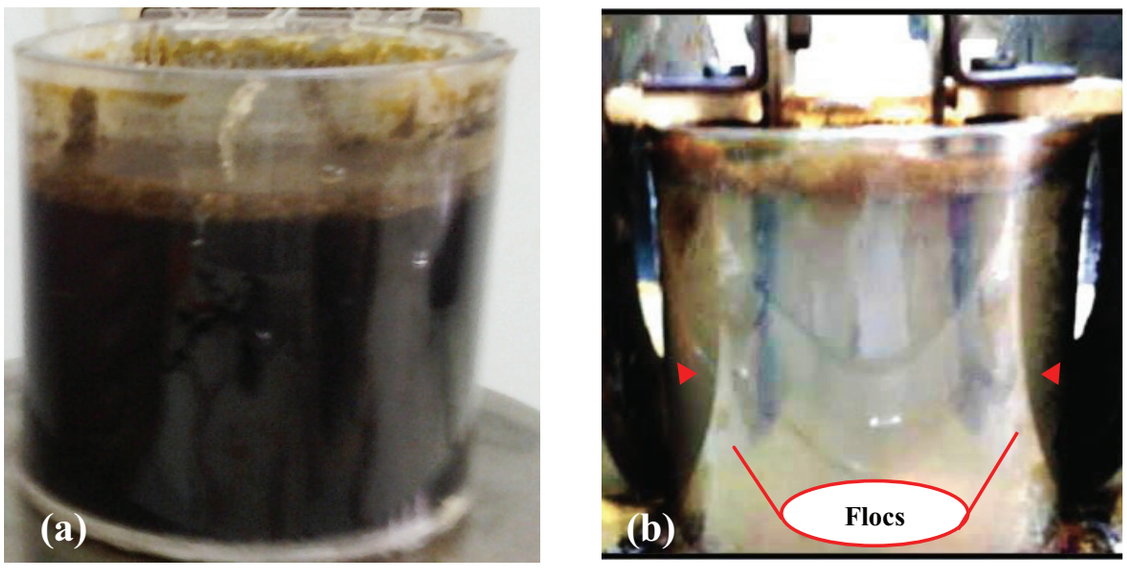

Fig. 9. The MO solution after the treatment by EC (a) and EC-MF (b).

Two mechanisms have been proposed to describe the formation of $Fe_2O_{3(s)}$ in an EC process involving iron electrodes [41,42]:

Mechanism I (4 < pH < 7)

Anode:

$$2Fe_{(s)} + H_2O_{(l)} \rightarrow 2Fe(OH)_{2(aq)} + 4H^+ + 4e^- \quad (3)$$

Bulk of solution:

$$2Fe(OH)_{2(aq)} + \tfrac{1}{2}O_{2(aq)} + H_2O_{(l)} \rightarrow 2Fe(OH)_{3(s)} \quad (4)$$

$$2Fe(OH)_{3(s)} \rightarrow Fe_2O_{3(s)} + 3H_2O_{(l)} \quad (5)$$

Cathode:

$$4H^+_{(aq)} + 4e^- \rightarrow 2H_{2(g)} \quad (6)$$

Overall:

$$2Fe_{(s)} + \tfrac{1}{2}O_{2(aq)} \rightarrow 2Fe_2O_{3(s)} + 2H_{2(g)} + 3H_2O_{(l)} \quad (7)$$

Mechanism II (4 < pH < 9)

Anode:

$$2Fe_{(s)} + 6H_2O_{(l)} \rightarrow 2Fe(OH)_{3(aq)} + 6H^+ + 6e^- \quad (8)$$

Bulk of solution:

$$2Fe(OH)_{3(s)} \rightarrow Fe_2O_{3(s)} + 3H_2O_{(l)} \quad (9)$$

Cathode:

$$6H^+ + 6e^- \rightarrow 3H_{2(g)} \quad (10)$$

Overall:

$$2Fe_{(s)} + 3H_2O_{(l)} \rightarrow Fe_2O_{3(s)} + 3H_{2(g)} \quad (11)$$

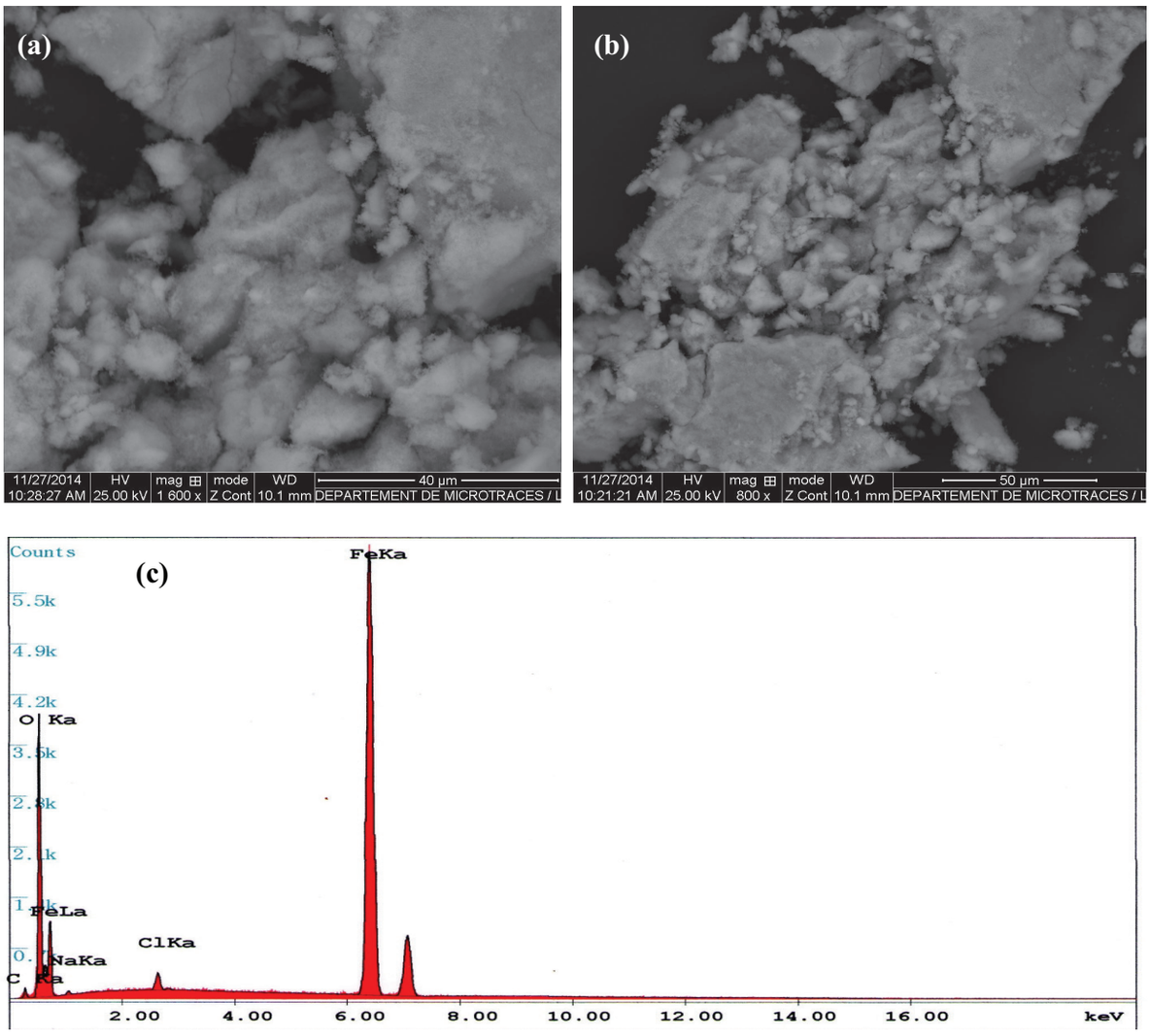

Fig. 10. SEM ((a) and (b)) and EDX (c) of the flocs generated by EC with application of the MF process with optimum conditions (C_{MO} = 15 mg/L, C_{NaCl} = 1.6 g/L, MF = 0.1 T, J = 64 A/m^2, d = 2 cm, t_{EC} = 30 min, pH = 7.25).

Table 1
Quantitative composition for atomic (At) and weight (Wt) percentage of the elements present in the floc generated by EC with the application of MF

Elements	Wt (%)	At (%)
Fe	60.84	30.56
O	34.49	60.47
Na	0.57	0.70
Cl	0.85	0.67
C	3.26	7.61

Furthermore, another strong oxidant of hypochlorite may be produced in a CE containing chlorides; the active chlorine can also enhance the oxidation of dye (13), resulting in enhancement of decolourization [40,43–47]:

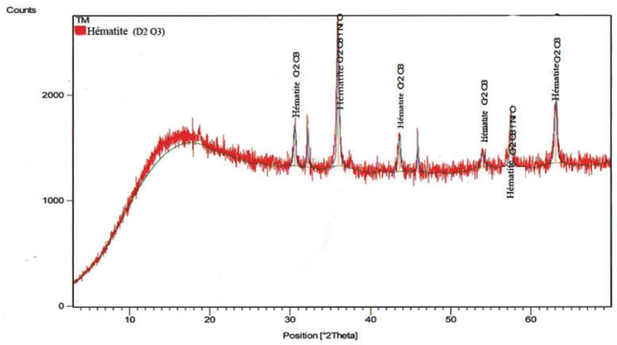

Fig. 11. XRD of the flocs generated by EC-MF process at the optimum conditions (C_{MO} = 15 mg/L, C_{NaCl} = 1.6 g/L, MF = 0.1 T, J = 64 A/m^2, d = 2 cm, t_{EC} = 30 min, pH = 7.25).

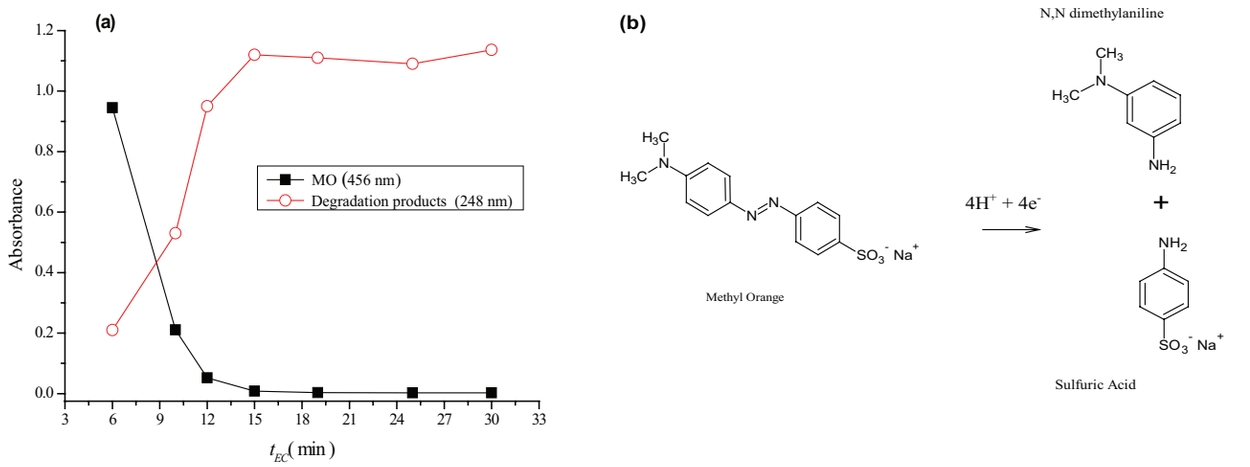

Fig. 12. (a) Evolution of the absorbance of MO and degradation products as a function of time (C_{MO} = 15 mg/L, C_{NaCl} = 1.6 g/L, MF = 0.1 T, J = 64 A/m², d = 2 cm, t_{EC} = 30 min, pH = 7.25). (b) Mechanism of the degradation of MO (C_{MO} = 15 mg/L, C_{NaCl} = 1.6 g/L, MF = 0.1 T, J = 64 A/m², d = 2 cm, t_{EC} = 30 min, pH = 7.25).

$$2Cl^-_{(aq)} \rightarrow Cl_{2(g)} + 2e^- \quad (12)$$

$$Cl_{2(g)} + H_2O_{(l)} \rightarrow HOCl_{(aq)} + H^+ + Cl^-_{(aq)} \quad (13)$$

$$HOCl + 2Fe^{2+} \rightarrow 2Fe^{3+} + Cl^- + OH^- \quad (14)$$

$$MO + HOCl \rightarrow \text{oxidized MO} + 2Cl^- \quad (15)$$

First pathway for decolourization of MO:

$$MO \rightarrow \text{Sulfanilic acid} + \text{2-naphtol} \quad (16)$$

$$Fe_2O_3 + \text{Sulfanilic acid} \rightarrow \text{Flocs} \quad (17)$$

Second pathway for decolourization of MO:

$$MO + HOCl \rightarrow \text{Chemical degradation} \quad (18)$$

6. Conclusions

The present investigation reveals that the EC process, with the application of MF, using iron electrodes can be used for the removal of dye molecules. The following conclusions can be drawn.

1. The experimental conditions for decolourization of MO by the EC-MF process have been optimized: C_{MO} = 15 mg/L, C_{NaCl} = 1.6 g/L, MF = 0.1 T, J = 64 A/m², initial pH 7.25, and d = 2 cm. Under these conditions, the removal efficiency reached 95% at 12 min. This rate is higher than that obtained with treatment by EC alone, which does not exceed 74%.
2. The XRD analysis proved that the formed flocs are crystalline in nature and the spectrum mainly indicated the presence of hematite Fe_2O_3. The SEM/EDX analysis of the flocs confirmed the presence of iron and oxygen. The MO removal mechanism proposed that MO is reduced to sulfanilic acid and 2-naphtol.
3. The energy consumption was decreased from 28 to 19 kWh/kg of MO, for the EC process and EC-MF, respectively.
4. The obtained results illustrate that the application of the MF in the EC process is one of the most promising methods for increasing removal efficiency, accentuating process compactness and lowering energy consumption. More research is still needed to open the process to industrial application perspectives.

References

[1] M. Fernández-Fernández, M.Á. Sanromán, D. Moldes, Recent developments and applications of immobilized laccase, Biotechnol. Adv., 31 (2013) 1808–1825.
[2] J. Huang, S. Chu, J. Chen, Y. Chen, Z. Xie, Enhanced reduction of an azo dye using henna plant biomass as a solid-phase electron donor, carbon source, and redox mediator, Biores. Technol., 161 (2014) 465–468.
[3] X. Quan, X. Zhang, H. Xu, In-situ formation and immobilization of biogenic nanopalladium into anaerobic granular sludge enhances azo dyes degradation, Water Res., 78 (2015) 74–83.
[4] S. Asad, M.A. Amoozegar, A.A. Pourbabaee, M.N. Sarbolouki, S.M.M. Dastgheib, Decolorization of textile azo dyes by newly isolated halophilic and halotolerant bacteria, Biores. Technol., 98 (2007) 2082–2088.
[5] R.L. Singh, P.K. Singh, R.P. Singh, Enzymatic decolorization and degradation of azo dyes - A review, Int. Biodeter. Biodegr., 104 (2015) 21–31.
[6] K.-C. Chen, J.-Y. Wu, D.-J. Liou, S.-C.J. Hwang, Decolorization of the textile dyes by newly isolated bacterial strains, J. Biotechnol., 101 (2003) 57–68.
[7] Y. Fu, T. Viraraghanvan, Fungal decolorization of dye wastewaters: A review, Bioresour. Technol., 79 (2011) 251–262.
[8] A.M. Talarposhti, T. Donnelly, G.K. Andersonm, Colour removal from a simulated dye wastewater using a two-phase anaerobic packed bed reactor, Water Res., 35 (2001) 425–432.
[9] B. Al Aji, Y. Yavuz, A.S. Koparal, Electrocoagulation of heavy metals containing model wastewater using monopolar iron electrodes, Sep. Purif. Technol., 86 (2012) 248–254.

[10] N. Daneshvar, H. Arshassi-Sorkhabi, A. Tizpar, Decolorization of orange II by electrocoagulation method, Sep. Purif. Technol., 31 (2003) 153–162.
[11] A. Gürses, M. Yalçin, C. Doğar, Electrocoagulation of some reactive dyes: A statistical investigation of some electrochemical variables, Waste Manage., 22 (2002) 491–499.
[12] M. Kobya, E. Demirbas, O.T. Can, M. Bayramoglu, Treatment of levafix orange textile dye solution by electrocoagulation, J. Hazard. Mater., 132 (2006) 183–188.
[13] P.K. Holt, G.W. Barton, C.A. Mitchell, The future for electrocoagulation as a localized water treatment technology, Chemosphere, 59 (2005) 355–367.
[14] G.B. Raju, M.T. Karuppiah, S.S. Latha, S. Parvathy, S. Prabhakar, Treatment of wastewater from synthetic textile industry by electrocoagulation–electrooxidation, Chem. Eng., 144 (2008) 51–58.
[15] D. Ghernaout, S. Irki, A. Boucherit, Removal of Cu^{2+} and Cd^{2+}, and humic acid and phenol by electrocoagulation using iron electrodes, Desalin. Water Treat., 52 (2014) 3256–3270.
[16] N. Mameri, A.R. Yeddou, H. Lounici, D. Belhocine, H. Grib, B. Bariou, Defluoridation of Septentrional Sahara water of North Africa by electrocoagulation process using bipolar aluminium electrodes, Water Res., 32 (1998) 1604–1612.
[17] D. Ghernaout, A.I. Al-Ghonamy, N. Ait Messaoudene, M. Aichouni, M.W. Naceur, F.Z. Benchelighem, A. Boucherit, Electrocoagulation of Direct Brown 2 (DB) and BF Cibacete Blue (CB) using aluminum electrodes, Sep. Sci. Technol., 50 (2015) 1413–1420.
[18] D. Ghernaout, M.W. Naceur, B. Ghernaout, A review of electrocoagulation as a promising coagulation process for improved organic and inorganic matters removal by electrophoresis and electroflotation, Desal. Water Treat., 28 (2011) 287–320.
[19] D. Ghernaout, Advanced oxidation phenomena in the electrocoagulation process: A myth or a reality? Desal. Water Treat., 51 (2013) 7536–7554.
[20] E. Pajootan, M. Arami, N.M. Mahmoodi, Binary system dye removal by electrocoagulation from synthetic and real colored wastewaters, J. Taiwan Inst. Chem. Eng., 43 (2012) 282–290.
[21] B. Al Aji, Y. Yavuz, A.S. Koparal, Electrocoagulation of heavy metals containing model wastewater using monopolar iron electrodes, Sep. Purif. Technol., 86 (2012) 248–254.
[22] S. Khoufi, F. Feki, S. Sayadi, Detoxification of olive mill wastewater by electrocoagulation and sedimentation processes, J. Hazard. Mater., 142 (2007) 58–67.
[23] F. Bouhezila, M. Hariti, H. Lounici, N. Mameri, Treatment of the OUED SMAR town landfill leachate by an electrochemical reactor, Desalination, 280 (2011) 347–353.
[24] W. Chu, C.-W. Ma, Quantitative prediction of direct and indirect dye ozonation kinetics, Water Res., 34 (2000) 3153–3160.
[25] S.H. Lin, C.H. Lai, Kinetic characteristics of textile wastewater ozonation in fluidized and fixed activated carbon beds, Water Res., 34 (2000) 763–772.
[26] V.C. Noninski, Magnetic field effect on copper electrodeposition in the Tafel potential region, Electrochim. Acta, 42 (1997) 251–254.
[27] R. Sueptitz, J. Koza, M. Uhlemann, A. Gebert, L. Schultz, Magnetic field effect on the anodic behaviour of a ferromagnetic electrode in acidic solutions, Electrochim. Acta, 54 (2009) 2229–2233.
[28] A. Bund, S. Koehler, H.H. Kuehnlein, W. Plieth, Magnetic field effects in electrochemical reactions, Electrochim. Acta, 49 (2003) 147–152.
[29] J.A. Koza, M. Uhlemann, A. Gebert, L. Schultz, The effect of magnetic fields on the electrodeposition of CoFe alloys, Electrochim. Acta, 53 (2008) 5344–5353.
[30] R. Sueptitz, K. Tschulik, M. Uhlemann, L. Schultz, A. Gebert, Magnetic field effect of high gradient magnetic fields on the anodic behaviour and localized corrosion of iron in sulphuric acid solutions, Corros. Sci., 53 (2011) 3222–3230.
[31] V.I. Beketov, V.Z. Parchinskii, N.B. Zorov, Effects of high-frequency electromagnetic treatment on the solid-phase extraction of aqueous benzene, naphthalene and phenol, J. Chromatogr. A, 731 (1996) 65–73.
[32] F. Alimi, M. Tlili, C. Gabrielli, G. Maurin, M. Ben Amor, Effect of a magnetic water treatment on homogeneous and heterogeneous precipitation of calcium carbonate, Water Res., 40 (2006) 1941–1950.
[33] C.J. Izquierdo, P. Canizares, M.A. Rodrigo, J.P. Leclerc, G. Valentin, F. Lapicque, Effect of the nature of the supporting electrolyte on the treatment of soluble oils by electrocoagulation, Desalination, 255 (2010) 15–20.
[34] D. Ghernaout, B. Ghernaout, From chemical disinfection to electrodisinfection: The obligatory itinerary? Desal. Water Treat., 16 (2010) 156–175.
[35] L. Holysz, A. Szczes, E. Chibowski, Effects of a static magnetic field on water and electrolyte solutions, J. Colloid Interf. Sci., 316 (2007) 996–1002.
[36] D. Ghernaout, B. Ghernaout, A. Boucherit, M.W. Naceur, A. Khelifa, A. Kellil, Study on mechanism of electrocoagulation with iron electrodes in idealized conditions and electrocoagulation of humic acids solution in batch using aluminium electrodes, Desal. Water Treat., 8 (2009) 91–99.
[37] D. Ghernaout, B. Ghernaout, A. Saiba, A. Boucherit, A. Kellil, Removal of humic acids by continuous electromagnetic treatment followed by electrocoagulation in batch using aluminium electrodes, Desalination, 239 (2009) 295–308.
[38] D. Ghernaout, B. Ghernaout, A. Kellil, Natural organic matter removal and enhanced coagulation as a link between coagulation and electrocoagulation, Desal. Water Treat., 2 (2009) 203–222.
[39] D. Ghernaout, M.W. Naceur, A. Aouabed, On the dependence of chlorine by-products generated species formation of the electrode material and applied charge during electrochemical water treatment, Desalination, 270 (2011) 9–22.
[40] D. Ghernaout, B. Ghernaout, A. Saiba, A. Boucherit, A. Kellil, Removal of humic acids by continuous electromagnetic treatment followed by electrocoagulation in batch using aluminium electrodes, Desalination, 239 (2009) 295–308.
[41] I.A. Şengil, M. Özacar, The decolorization of C.I. Reactive Black 5 in aqueous solution by electrocoagulation using sacrificial iron electrodes, J. Hazard. Mater., 161 (2009) 1369–1376.
[42] H.A. Moreno-Casillas, D.L. Cocke, J.A.G. Gomes, P. Morkovsky, J.R. Parga, E. Peterson, Electrocoagulation mechanism for COD removal, Sep. Purif. Technol., 56 (2007) 204–211.
[43] S.-H. Chang, K.-S. Wang, H.-H. Liang, H.-Y. Chen, H.-C. Li, T.-H. Peng, Y.-C. Su, C.-Y. Chang, Treatment of Reactive Black 5 by combined electrocoagulation–granular activated carbon adsorption–microwave regeneration process, J. Hazard. Mater., 175 (2010) 850–857.
[44] S. Kourdali, A. Badis, A. Saiba, A. Boucherit, H. Boutoumi, Humic acid removal by electrocoagulation using aluminium sacrificial anode under influencing operational parameters, Desal. Water Treat., 52 (2014) 5442–5453.
[45] E. Gatsios, J.N. Hahladakis, E. Gidarakos, Optimization of electrocoagulation (EC) process for the purification of a real industrial wastewater from toxic metals, J. Environ. Manage., 154 (2015) 117–127.
[46] A.S. Koparal, Y.Ş. Yildiz, B. Keskinler, N. Demircioğlu, Effect of initial pH on the removal of humic substancesfrom wastewater by electrocoagulation, Sep. Purif. Technol., 59 (2008) 175–182.
[47] M. Vlachou, J. Hahladakis, E. Gidarakos, Effect of various parameters in removing Cr and Ni from model wastewater by using electrocoagulation, Global NEST J., 15 (2013) 494–503.